HL-LHC and e^+e^- inputs to global fits

EF03 Heavy flavor and top

18th November 2021

V. Miralles,[1] M. Miralles López,[1] M. Moreno Llácer,[1] A. Peñuelas,[1,2] M. Perelló,[1] M. Vos,[1]

Based on arXiv:1907.10619, arXiv:2006.14631 and arXiv:2107.13917

[1] Universitat de València and CSIC, [2] U.Mainz, Prisma

Introduction

- As the top quark was not produced in LEP its EW sector could not be precisely measured until now
- The LHC data allows, finally, for precise measurements of this sector
- Here we present results of a global fit to top-quark EW couplings
- We used the most recent available data from the LHC (ATLAS and CMS), and also from LEP and Tevatron
- We include the QCD corrections at NLO on most of the observables used
- The fits have been performed using `HEPfit` [1910.14012]
- Estimations on the improvement of the measurements are presented for the HL-LHC
- Estimation for the relevant observables for this fit in a future e^+e^- colliders are shown
- Prospects for our limits in the HL-LHC and a future e^+e^- colliders are obtained

Theoretical Framework

- We use an EFT description to parametrise deviations from the SM

$$\mathscr{L}_{\text{eff}} = \mathscr{L}_{\text{SM}} + \frac{1}{\Lambda^2}\sum_i C_i O_i + \mathscr{O}\left(\Lambda^{-4}\right)$$

- The Wilson coefficients can be interpreted in terms of NP mediators
- We include Λ^{-2} terms from the interference between the SM and D6
- We also include Λ^{-4} operators arising from squaring the D6
- The effects of D8 operators, contributing to the same Λ^{-4} order, are omitted

$$\sigma = \sigma_{\text{SM}} + \underbrace{\frac{1}{\Lambda^2}\sum C_i O_i}_{\text{SM }\times\text{D6}} + \underbrace{\left(\frac{1}{\Lambda^2}\sum C_i O_i\right)\left(\frac{1}{\Lambda^2}\sum C_j O_j\right)}_{\text{D6}\times\text{D6}} + \underbrace{O(1/\Lambda^4)}_{\text{SM }\times\text{D8}}$$

- We only consider the EW two-fermion operators and ignore the imaginary parts
- The four-fermion operators are ignored

EW top-quark EFT Basis

Left and right-handed couplings of the t- and b-quark to the Z

$$O^3_{\varphi Q} \equiv \frac{1}{2}\left(\bar{q}\tau^I\gamma^\mu q\right)\left(\varphi^\dagger i\overleftrightarrow{D}^I_\mu\,\varphi\right)$$
$$O^1_{\varphi Q} \equiv \frac{1}{2}\left(\bar{q}\gamma^\mu q\right)\left(\varphi^\dagger i\overleftrightarrow{D}_\mu\varphi\right)$$
$$O_{\varphi u} \equiv \frac{1}{2}\left(\bar{u}\gamma^\mu u\right)\left(\varphi^\dagger i\overleftrightarrow{D}_\mu\varphi\right)$$
$$O_{\varphi d} \equiv \frac{1}{2}\left(\bar{d}\gamma^\mu d\right)\left(\varphi^\dagger i\overleftrightarrow{D}_\mu\varphi\right)$$

EW dipole operators

$$O_{uW} \equiv \left(\bar{q}\tau^I\sigma^{\mu\nu}u\right)\left(\varepsilon\varphi^* W^I_{\mu\nu}\right)$$
$$O_{dW} \equiv \left(\bar{q}\tau^I\sigma^{\mu\nu}d\right)\left(\varphi W^I_{\mu\nu}\right)$$
$$O_{uB} \equiv \left(\bar{q}\sigma^{\mu\nu}u\right)\left(\varepsilon\varphi^* B_{\mu\nu}\right)$$
$$O_{dB} \equiv \left(\bar{q}\sigma^{\mu\nu}d\right)\left(\varphi B_{\mu\nu}\right)$$

Chromo magnetic dipole operators

$$O_{uG} \equiv \left(\bar{q}\sigma^{\mu\nu}T^A u\right)\left(\varepsilon\varphi^* G^A_{\mu\nu}\right)$$
$$O_{dG} \equiv \left(\bar{q}\sigma^{\mu\nu}T^A d\right)\left(\varphi G^A_{\mu\nu}\right)$$

Top/Bottom yukawa

$$O_{u\varphi} \equiv \left(\bar{q}u\right)\left(\varepsilon\varphi^*\ \varphi^\dagger\varphi\right)$$
$$O_{d\varphi} \equiv \left(\bar{q}d\right)\left(\varphi\ \varphi^\dagger\varphi\right)$$

Charged current interaction

$$O_{\varphi ud} \equiv \frac{1}{2}\left(\bar{u}\gamma^\mu d\right)\left(\varphi^T\varepsilon i D_\mu\varphi\right)$$

- Rotation of Warsaw basis following [1802.07237] (LHC Top WG)

$$O^1_{\varphi Q} \to O^-_{\varphi Q} = O^1_{\varphi Q} - O^3_{\varphi Q}; \qquad O_{xB} \to O_{xZ} = -\sin\theta_W O_{xB} + \cos\theta_W O_{xW}$$

Methods & Data

- Dependence of the observables calculated at NLO in QCD with the Monte Carlo generator `MG5_aMC@NLO` [JHEP 07 (2014) 079]
- `SMEFT@NLO` [arXiv:2008.11743] UFO model was used except for C_{bW}, $C_{\varphi tb}$, C_{bZ} and $C_{\varphi b}$ where the `TEFT_EW` [JHEP 05 (2016) 052] UFO model was used
- The fit is performed as a Bayesian statistical analysis of the model using the open source `HEPfit` [1910.14012]

Process	Observable	$\sqrt{s}$	$\int \mathcal{L}$	Experiment
$pp \to t\bar{t}H$	cross section	13 TeV	140 fb^{-1}	ATLAS
$pp \to t\bar{t}W$	cross section	13 TeV	36 fb^{-1}	CMS
$pp \to t\bar{t}Z$	(differential) x-sec.	13 TeV	140 fb^{-1}	ATLAS
$pp \to t\bar{t}\gamma$	(differential) x-sec.	13 TeV	140 fb^{-1}	ATLAS
$pp \to tZq$	cross section	13 TeV	140 fb^{-1}	CMS
$pp \to t\gamma q$	cross section	13 TeV	36 fb^{-1}	CMS
$pp \to tb$ (s-ch)	cross section	8 TeV	20 fb^{-1}	ATLAS+CMS
$pp \to tW$	cross section	8 TeV	20 fb^{-1}	ATLAS+CMS
$pp \to tq$ (t-ch)	cross section	8 TeV	20 fb^{-1}	ATLAS+CMS
$t \to W^+b$	F_0, F_L	8 TeV	20 fb^{-1}	ATLAS+CMS
$p\bar{p} \to t\bar{b}$ (s-ch)	cross section	1.96 TeV	9.7 fb^{-1}	Tevatron
$e^-e^+ \to b\bar{b}$	R_b , A^{bb}_{FBLR}	$\sim$ 91 GeV	202.1 pb^{-1}	LEP

Sensitivity

- The observables and coefficients in red are not included
- The $pp \to t\bar{t}$ process is omitted in the fit in order to be consistent as it is used to reduce the dependence of $pp \to t\bar{t}X$ on Wilson coefficients that have not been included.

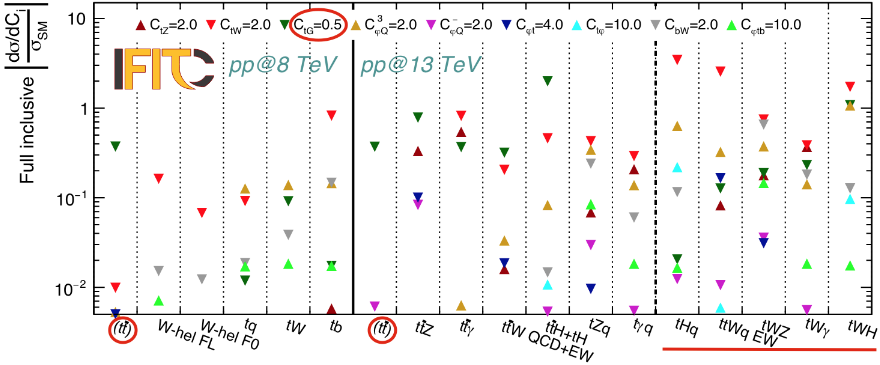

Results - Sensitivity Individual Constraints

- Good interplay between the parameters and chosen observables
- The differential cross sections (darker regions) provide the best constraints for some observables

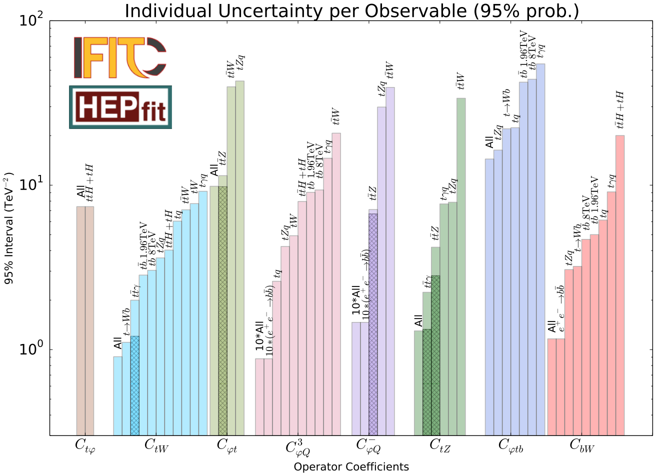

Results - Differential Cross Section Effect

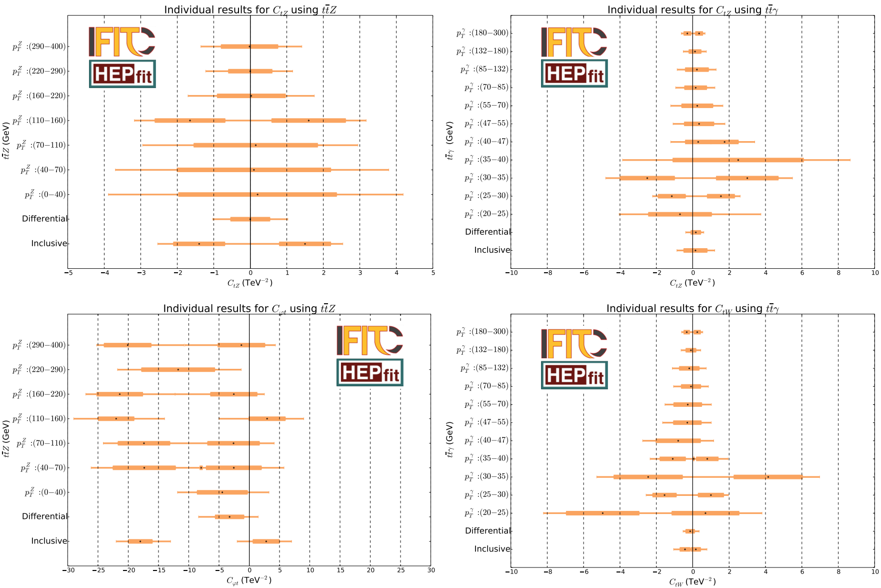

Results - Complementarity Between Observables

- Very good complementarity between the observables
- The global fit marginalised limit is quite close to the intersection of individual fits → The data set is diverse enough to avoid the existence of blind directions

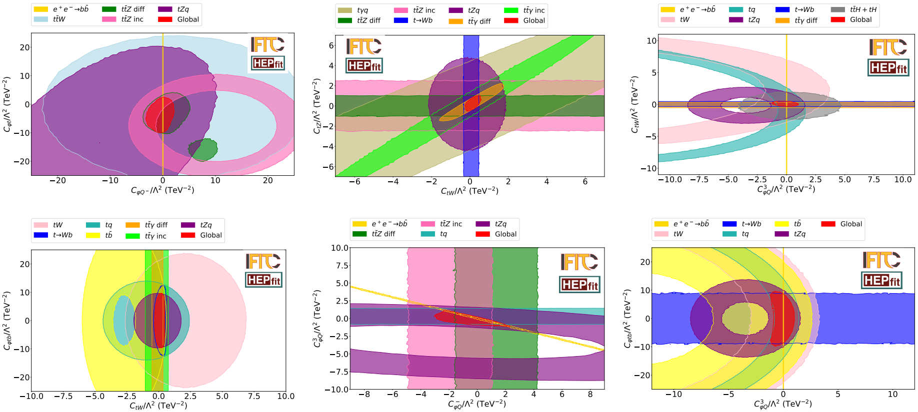

Results - Global Fit

- The constraints of the linear (only Λ^{-2} terms) global fit are similar to those of the quadratic ($\Lambda^{-2} + \Lambda^{-4}$ terms) global fit for most cases
- Estimation of the impact of correlations between the observables and the extension of our basis with 7 four-fermion operators and C_{tG}
- Robust Limit: Envelope found from combining all the results

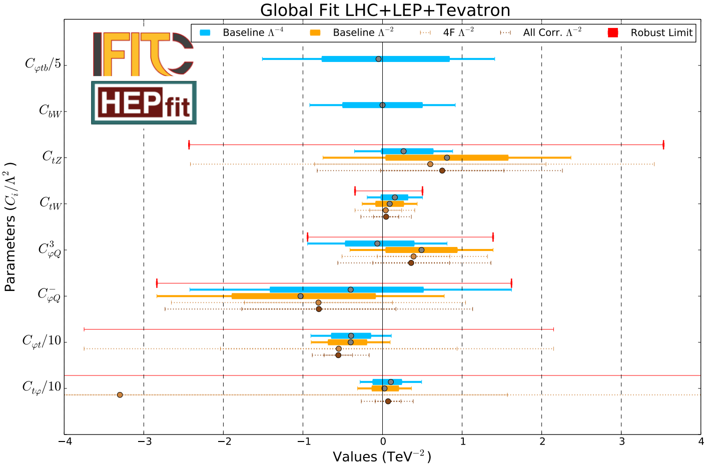

Results - Conclusions

- All the results are compatible with the SM with a 95% probability
- We find a reduction of the uncertainty of all the parameters of around a factor two with respect to our previous work [JHEP12(2019)098]
- Adding important correlations between the observables does not dramatically change the results, but increasing the basis has an effect
- LEP measurements provide tight bounds on several operators as the left-handed coupling $C^{-}_{\varphi Q}$ and $C^{(3)}_{\varphi Q}$
- The limits are quite robust even when we only consider linear terms, except for C_{bW}, $C_{\varphi tb}$ and C_{tZ}
- The addition of the differential cross sections of $pp \to t\bar{t}Z$ and $pp \to t\bar{t}\gamma$ have an important effect on C_{tZ} and $C_{\varphi t}$
- We find the most stringent bound on top EW couplings from an EFT including all relevant 2-fermions degrees of freedom (see [JHEP 04 (2019) 100], [JHEP 02 (2020) 131], [CMS-PAS-TOP-19-001])

Future Colliders - Prospects for Measurements at HL-LHC

Theoretical Uncertainties $\longrightarrow$ scale with $1/2$

Experimental Uncertainties $\begin{cases} \text{Modelling} \longrightarrow \text{scale with } 1/2 \\ \text{Systematic} \longrightarrow \text{scale with } 1/\sqrt{\mathscr{L}} \\ \text{Statistical} \longrightarrow \text{scale with } 1/\sqrt{\mathscr{L}} \end{cases}$

Future Colliders - Prospects for Measurements at HL-LHC

Inclusive cross sections and helicities

Process	Measured (fb)	SM (fb)	LHC Unc.					HL-LHC Unc.				
			theo.	exp.				theo.	exp.			
				stat.	sys.	mod.	tot.		stat.	sys.	mod.	tot.
$pp \to t\bar{t}H + tHq$	640	664.3	41.7	90	40	70.7	121.2	20.9	19.4	8.6	35.4	41.3
$pp \to t\bar{t}Z$	990	810.9	85.8	51.5	48.9	67.3	97.8	42.9	11.1	10.6	33.6	37.0
$pp \to t\bar{t}\gamma$	39.6	38.5	1.76	0.8	1.25	2.16	2.62	0.88	0.17	0.27	1.08	1.13
$pp \to tZq$	111	102	3.5	13.0	6.1	6.2	15.7	1.75	2.09	0.98	3.1	3.87
$pp \to t\gamma q$	115.7	81	4	17.1	21.1	21.1	34.4	2	1.9	2.3	10.6	11.0
$pp \to t\bar{t}W + \text{EW}$	770	647.5	76.1	120	59.6	73.0	152.6	38.1	13.1	6.5	36.5	39.4
$pp \to t\bar{b}$ (s-ch)	4900	5610	220	784	936	790	1454	110	35	42	395	399
$pp \to tW$	23100	22370	1570	1086	2000	2773	3587	785	49	89	1386	1390
$pp \to tq$ (t-ch)	87700	84200	250	1140	3128	4766	5810	125	51	140	2383	2390
F_0	0.693	0.687	0.005	0.009	0.006	0.009	0.014	0.003	0.0004	0.0003	0.004	0.004
F_L	0.315	0.311	0.005	0.006	0.003	0.008	0.011	0.003	0.0003	0.0002	0.004	0.004

Table: The data shown is the inclusive cross-section written in fb for all the channels except, obviously, for the W Helicities (F_0 and F_L).

Future Colliders - Prospects for Measurements at HL-LHC

$pp \to t\bar{t}Z$ differential cross section

$pp \to t\bar{t}Z$	Measured ($\text{fb} \cdot \text{GeV}^{-1}$)	SM ($\text{fb} \cdot \text{GeV}^{-1}$)	LHC Unc.					HL-LHC Unc.				
			theo.	exp.				theo.	exp.			
				stat.	sys.	mod.	tot.		stat.	sys.	mod.	tot.
p_T^Z : (0-40)	1.47	2.21	0.263	0.53	0.23	0.21	0.615	0.132	0.114	0.050	0.105	0.163
p_T^Z : (40-70)	4.32	4.59	0.543	0.94	0.60	0.51	1.223	0.272	0.203	0.130	0.253	0.349
p_T^Z : (70-110)	4.24	4.60	0.555	0.75	0.54	0.36	0.993	0.278	0.162	0.117	0.182	0.270
p_T^Z : (110-160)	4.4	3.45	0.429	0.55	0.43	0.39	0.800	0.215	0.118	0.093	0.197	0.248
p_T^Z : (160-220)	1.75	2.05	0.261	0.31	0.15	0.13	0.371	0.131	0.067	0.033	0.066	0.100
p_T^Z : (220-290)	0.58	1.03	0.130	0.16	0.047	0.034	0.174	0.065	0.035	0.010	0.017	0.041
p_T^Z : (290-400)	0.56	0.59	0.071	0.11	0.055	0.057	0.132	0.036	0.023	0.012	0.029	0.038

Table: We show the unfolded bin contents for the absolute parton-level differential cross-section measurement.

Future Colliders - Prospects for Measurements at HL-LHC

$pp \to t\bar{t}\gamma$ differential cross section

$pp \to t\bar{t}\gamma$	Measured ($\text{fb} \cdot \text{GeV}^{-1}$)	SM ($\text{fb} \cdot \text{GeV}^{-1}$)	LHC Unc.					HL-LHC Unc.				
			theo.	exp.				theo.	exp.			
				stat.	sys.	mod.	tot.		stat.	sys.	mod.	tot.
p_T^γ : (20-25)	1.782	1.670	0.066	0.116	0.168	0.108	0.231	0.033	0.025	0.036	0.054	0.070
p_T^γ : (25-30)	1.328	1.183	0.040	0.089	0.052	0.092	0.138	0.020	0.019	0.011	0.046	0.051
p_T^γ : (30-35)	0.966	0.8663	0.0302	0.072	0.026	0.060	0.097	0.0151	0.016	0.0056	0.030	0.0342
p_T^γ : (35-40)	0.705	0.6616	0.0205	0.058	0.015	0.042	0.0733	0.0103	0.0125	0.0032	0.021	0.0248
p_T^γ : (40-47)	0.474	0.4790	0.0160	0.04	0.0096	0.048	0.0629	0.0080	0.0086	0.0021	0.024	0.0254
p_T^γ : (47-55)	0.333	0.3464	0.0094	0.031	0.0067	0.017	0.0360	0.0047	0.0067	0.0014	0.0085	0.0109
p_T^γ : (55-70)	0.221	0.2188	0.0056	0.019	0.0038	0.0081	0.0210	0.0028	0.0041	0.00082	0.0041	0.0058
p_T^γ : (70-85)	0.122	0.1286	0.0031	0.014	0.0026	0.0069	0.0158	0.0016	0.0030	0.00056	0.0035	0.0046
p_T^γ : (85-132)	0.060	0.06037	0.0017	0.005	0.0014	0.0068	0.0086	0.00084	0.0011	0.00029	0.0034	0.0036
p_T^γ : (132-180)	0.020	0.02373	0.00077	0.003	0.00044	0.00080	0.00314	0.00039	0.00065	0.000095	0.00040	0.00077
p_T^γ : (180-300)	0.009	0.00790	0.00028	0.00045	0.000085	0.0014	0.00144	0.00014	0.000097	0.000018	0.00068	0.00069

Table: We show the unfolded bin contents for the absolute parton-level differential cross-section measurement.

Future Colliders - Complementarity on e^+e^- Colliders

Good complementarity between $b\bar{b}$ (LEP) and $t\bar{t}$ (future e^+e^- collider) if we reach $\sqrt{s} > 2m_t$

$$\delta g_L^t = -(C_{\varphi Q}^1 - C_{\varphi Q}^3) m_t^2/\Lambda^2$$

$$\delta g_L^b = -(C_{\varphi Q}^1 + C_{\varphi Q}^3) m_t^2/\Lambda^2$$

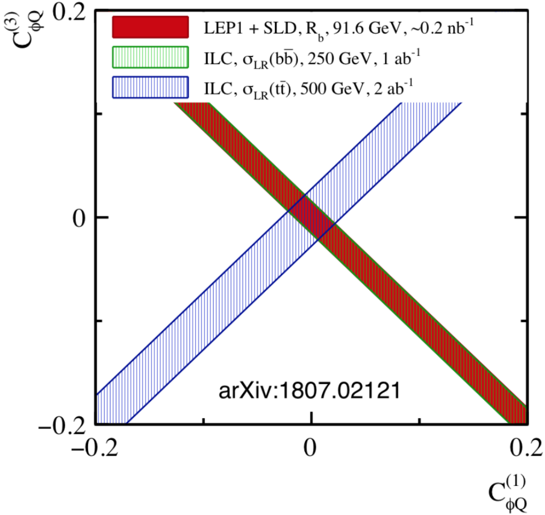

Future Colliders - Prospects for Measurements at e^+e^- Linear Collider

Process	Observable	$\sqrt{s}$	$\int \mathscr{L}$	Experiment
$e^+e^- \to b\bar{b}$	(+80%, -30%) x-section, A_{FB}^{bb}	250 GeV	2 ab^{-1}	ILC250
	(-80%, +30%) x-section, A_{FB}^{bb}	250 GeV	2 ab^{-1}	ILC250
	(+80%, -30%) x-section, A_{FB}^{bb}	500 GeV	4 ab^{-1}	ILC500
	(-80%, +30%) x-section, A_{FB}^{bb}	500 GeV	4 ab^{-1}	ILC500
	(+80%, -30%) x-section, A_{FB}^{bb}	1000 GeV	8 ab^{-1}	ILC1000
	(-80%, +30%) x-section, A_{FB}^{bb}	1000 GeV	8 ab^{-1}	ILC1000
$e^+e^- \to t\bar{t}$	optimal observables	500 GeV	4 ab^{-1}	ILC500
$e^+e^- \to t\bar{t}$	optimal observables	1000 GeV	8 ab^{-1}	ILC1000

Optimal Observables: minimise the determinant of the covariance matrix [1807.02121]

$$\frac{d\sigma}{d\Phi} = \frac{d\sigma_{\text{SM}}}{d\Phi} + \sum_i C_i \frac{d\sigma_i}{d\Phi}, \qquad \bar{O}_i = \varepsilon \mathscr{L} \int d\Phi \left(\frac{d\sigma_i}{d\Phi} \Big/ \frac{d\sigma_{\text{SM}}}{d\Phi} \right) \frac{d\sigma}{d\Phi}$$

Future Colliders - Prospects for Measurements at e^+e^- Linear Collider: ILC250

S. Bilokin, A. Irles, R. Pöschl and F. Richard, *in preparation*

$e^+e^- \to b\bar{b}$:

	Uncertainty	Correlation			
		LR x-section	LR A_{FB}^{bb}	RL x-section	RL A_{FB}^{bb}
LR x-section	5 fb	1	0.35	0.92	0.88
LR A_{FB}^{bb}	0.165	0.35	1	0.38	0.50
RL x-section	1.8 fb	0.92	0.38	1	0.97
RL A_{FB}^{bb}	0.214	0.88	0.50	0.97	1

Future Colliders - Prospects for Measurements at e^+e^- Linear Collider: ILC500

$e^+e^- \to b\bar{b}$:

S. Bilokin, et al.	Uncertainty
LR x-section	1.34 fb
LR A_{FB}^{bb}	0.19
RL x-section	0.74 fb
RL A_{FB}^{bb}	0.34

$e^+e^- \to t\bar{t}$:

[1807.02121]	Uncertainty	Correlation			
		$C_{\varphi t}$	$C_{\varphi Q}^-$	C_{tW}	C_{tB}
$C_{\varphi t}$	0.011	1	0.82	0.94	-0.91
$C_{\varphi Q}^-$	0.011	0.82	1	0.94	-0.93
C_{tW}	0.022	0.94	0.94	1	-0.97
C_{tB}	0.0076	-0.91	-0.93	-0.97	1

Future Colliders - Prospects for Measurements at e^+e^-
Linear Collider: ILC1000

$e^+e^- \to b\bar{b}$:

S. Bilokin, et al.	Uncertainty
LR x-section	0.74 fb
LR A_{FB}^{bb}	0.42
RL x-section	0.40 fb
RL A_{FB}^{bb}	0.78

$e^+e^- \to t\bar{t}$:

[1807.02121]	Uncertainty	Correlation							
		C_{et}	C_{eQ}	C_{lt}	C_{lQ}^-	$C_{\varphi Q}^-$	$C_{\varphi t}$	C_{tW}	C_{tB}
C_{et}	0.00053	1	-0.053	0	0	0	0	0	0
C_{eQ}	0.00053	-0.053	1	0	0	0	0	0	0
C_{lt}	0.0005	0	0	1	-0.18	0	0	0	0
C_{lQ}^-	0.0005	0	0	-0.18	1	0	0	0	0
$C_{\varphi Q}^-$	0.087	0	0	0	0	1	0.31	0	0
$C_{\varphi t}$	0.087	0	0	0	0	0.31	1	0	0
C_{tW}	0.00905	0	0	0	0	0	0	1	-0.85
C_{tB}	0.0052	0	0	0	0	0	0	-0.85	1

Future Colliders - Prospects for EW Top-Quark Couplings

- Results from [JHEP12(2019)098] show the extraordinary impact of adding the data from a e^+e^- collider working at 500 GeV $\rightarrow$ It is crucial to go $\sqrt{s} > 2m_t$
- The LHC Run 2 data here refers to the data available in mid 2019, with the current data the errors are reduced around a factor two

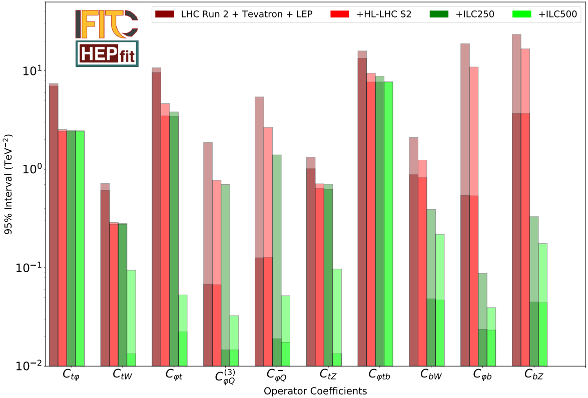

Future Colliders - Prospects for EW Top-Quark Couplings + $e^+e^- Q\bar{Q}$

Only constrained with data at two $\sqrt{s} > 2m_t$:

$$\begin{aligned}
O_{lQ}^1 &\equiv \tfrac{1}{2}\ \bar{Q}\gamma_\mu Q\,\bar{l}\gamma^\mu l\\
O_{lQ}^3 &\equiv \tfrac{1}{2}\ \bar{q}\tau^I\gamma_\mu q\,\bar{l}\tau^I\gamma^\mu l\\
O_{lt} &\equiv \tfrac{1}{2}\ \bar{t}\gamma_\mu t\,\bar{l}\gamma^\mu l\\
O_{lb} &\equiv \tfrac{1}{2}\ \bar{b}\gamma_\mu b\,\bar{l}\gamma^\mu l\\
O_{eQ} &\equiv \tfrac{1}{2}\ \bar{Q}\gamma_\mu Q\,\bar{e}\gamma^\mu e\\
O_{et} &\equiv \tfrac{1}{2}\ \bar{t}\gamma_\mu t\,\bar{e}\gamma^\mu e\\
O_{eb} &\equiv \tfrac{1}{2}\ \bar{b}\gamma_\mu b\,\bar{e}\gamma^\mu e
\end{aligned}$$

	10-parameter fit ILC250 + ILC500	17-parameter fit + ILC1000
$C_{\varphi t}/\Lambda^2$	0.037	0.021
$C_{\varphi Q}^3/\Lambda^2$	0.020	0.017
$C_{\varphi Q}^-/\Lambda^2$	0.036	0.021
C_{tW}/Λ^2	0.071	0.030
C_{tZ}/Λ^2	0.074	0.032
$C_{t\varphi}/\Lambda^2$	1.735	1.735
$C_{\varphi b}/\Lambda^2$	0.030	0.047
C_{bW}/Λ^2	0.204	0.478
C_{bZ}/Λ^2	0.163	0.438
$C_{\varphi tb}/\Lambda^2$	3.90	3.67
C_{eu}/Λ^2	—	0.0021
C_{ed}/Λ^2	—	0.0032
C_{eq}/Λ^2	—	0.0019
C_{lu}/Λ^2	—	0.0020
C_{ld}/Λ^2	—	0.0100
C_{lq}^-/Λ^2	—	0.0020
C_{lq}^+/Λ^2	—	0.0039

Future Colliders - Prospects for Top-Quark+Higgs Sector

For current limits on this sector look at [2012.02779] and [1910.03606]

- The determination of the Higgs boson couplings at ILC250 is degraded by the additional top-quark operators
- We can recover the original bounds by the inclusion of precise measurements of top-quark EW couplings at the LHC
- The physical Higgs couplings are relatively robust, as the top mass is larger than the energy scale of EW processes
- If the ILC reaches 500 GeV it will provide very precise constraints on the top operators

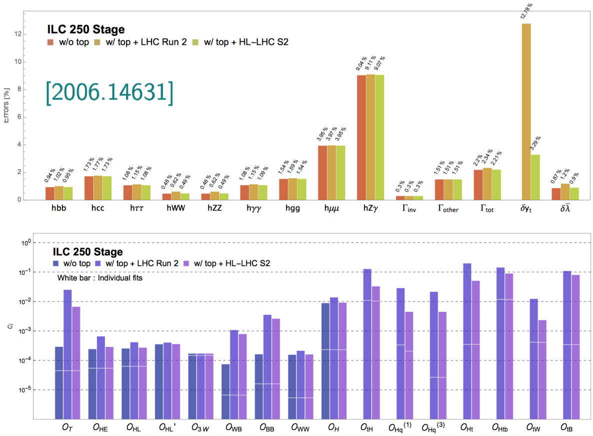

Summary

- Current data allows for constraining the top-quark EW considering only Λ^{-2} terms
- Λ^{-4} terms are specially relevant for C_{bW} and $C_{\varphi tb}$ whose Λ^{-2} dependence vanishes in the limit $m_b \to 0$
- The correlation between observables does not seem to have a dramatic impact in the final result
- Including additional operators has an important effect on some (but not all) of the limits
- In the HL-LHC the theoretical and modelling uncertainties are dominant $\to$ hinders the improvement on the limits
- To improve the limits in some order of magnitudes it is crucial to build a e^+e^- collider working at $\sqrt{s} > 2m_t$
- An e^+e^- collider working at two different energies above $2m_t$ is needed to constrain $e^+e^-Q\bar{Q}$
- For a precise fit on the combined sector of the top plus the Higgs it could be enough with the data of a e^+e^- collider working at $\sqrt{s} = 250$ GeV given the expected precision that the LHC could achieve for the top-quark EW couplings

Thank you!

Back up

Numerical values for the Wilson Coefficients

	Linear+Quadratic (95% probability intervals)		
C/Λ^2 (TeV^{-2})	Individual	Global-Baseline	Global-Robust
$C_{t\varphi}$	[-3.05, 4.05]	[-2.82, 4.92]	[-121.82, 62.82]
$C_{\varphi Q}^{-}$	[-0.038, 0.079]	[-2.42, 1.62]	[-2.84, 1.62]
$C_{\varphi Q}^{3}$	[-0.019, 0.040]	[-0.94, 0.81]	[-0.94, 1.39]
$C_{\varphi t}$	[-8.6, 1.5]	[-9.01, 1.11]	[-37.50, 21.50]
C_{tW}	[-0.28, 0.32]	[-0.19, 0.50]	[-0.35, 0.50]
C_{tZ}	[-0.39, 0.57]	[-0.35, 0.88]	[-2.43, 3.53]
$C_{\varphi tb}$	[-6.61, 6.71]	[-7.55, 7.05]	–
C_{bW}	[-0.47, 0.47]	[-0.91, 0.91]	–

Table: Allowed ranges of the Wilson coefficients with a probability of 95% expressed in TeV^{-2} including linear and quadratic terms. We show, from left to right, the results of three fits: individual, global baseline and global robust. The robust result accounts for the effects of the correlations between the observables, the inclusion of further operators and the theoretical uncertainties on the parameterisations.

Back up

Numerical values for the Wilson Coefficients

C/Λ^2 (TeV^{-2})	Linear (95% probability intervals)	
	Individual	Global-Baseline
$C_{t\varphi}$	[-3.17, 3.47]	[-3.13, 3.63]
$C^{-}_{\varphi Q}$	[-0.038, 0.079]	[-2.84, 0.78]
$C^{3}_{\varphi Q}$	[-0.019, 0.040]	[-0.41, 1.39]
$C_{\varphi t}$	[-6.6, 1.8]	[-8.96, 0.96]
C_{tW}	[-0.30, 0.38]	[-0.26, 0.44]
C_{tZ}	[-0.82, 2.21]	[-0.75, 2.37]

Table: Allowed ranges of the Wilson coefficients with a probability of 95% expressed in TeV^{-2} including only linear terms. We show, from left to right, the results of three fits: individual, global baseline and global robust. The robust result accounts for the effects of the correlations between the observables, the inclusion of further operators and the theoretical uncertainties on the parameterisations.

Back up

4-fermion operators

$C_{qq}^{1(ijkl)}$ $C_{uu}^{(ijkl)}$ $C_{qu}^{8(ijkl)}$	$(\bar{q}_i\gamma^\mu q_j)(\bar{q}_k\gamma_\mu q_l)$ $(\bar{u}_i\gamma^\mu u_j)(\bar{u}_k\gamma_\mu u_l)$ $(\bar{q}_i\gamma^\mu T^A q_j)(\bar{u}_k\gamma_\mu T^A u_l)$	$C_{qq}^{3(ijkl)}$ $C_{ud}^{8(ijkl)}$ $C_{qd}^{8(ijkl)}$	$(\bar{q}_i\tau^I\gamma^\mu q_j)(\bar{q}_k\tau^I\gamma_\mu q_l)$ $(\bar{u}_i\gamma^\mu T^A u_j)(\bar{d}_k\gamma_\mu T^A d_l)$ $(\bar{q}_i\gamma^\mu T^A q_j)(\bar{d}_k\gamma_\mu T^A d_l)$
C_{tu}^8	$\sum_{i=1,2} 2C_{uu}^{(i33i)}$	C_{td}^8	$\sum_{i=1,2,3} C_{ud}^{8(33ii)}$
C_{Qu}^8	$\sum_{i=1,2} C_{qu}^{8(33ii)}$	$C_{Qq}^{1,8}$	$\sum_{i=1,2} C_{qq}^{1(i33i)} + 3C_{qq}^{3(i33i)}$
C_{Qd}^8	$\sum_{i=1,2,3} C_{qd}^{8(33ii)}$	$C_{Qq}^{3,8}$	$\sum_{i=1,2} C_{qq}^{1(i33i)} - C_{qq}^{3(i33i)}$
–	–	C_{tq}^8	$\sum_{i=1,2} C_{uq}^{8(ii33)}$

Back up

Dependencies [1910.03606] :

parameter	$t\bar{t}$	single t	tW	tZ	t decay	$t\bar{t}Z$	$t\bar{t}W$
$C_{Qq}^{1,8}$	Λ^{-2}	–	–	–	–	Λ^{-2}	Λ^{-2}
$C_{Qq}^{3,8}$	Λ^{-2}	Λ^{-4} $[\Lambda^{-2}]$	–	Λ^{-4} $[\Lambda^{-2}]$	Λ^{-4} $[\Lambda^{-2}]$	Λ^{-2}	Λ^{-2}
C_{tu}^{8}, C_{td}^{8}	Λ^{-2}	–	–	–	–	Λ^{-2}	–
$C_{Qq}^{1,1}$	Λ^{-4} $[\Lambda^{-2}]$	–	–	–	–	Λ^{-4} $[\Lambda^{-2}]$	Λ^{-4} $[\Lambda^{-2}]$
$C_{Qq}^{3,1}$	Λ^{-4} $[\Lambda^{-2}]$	Λ^{-2}	–	Λ^{-2}	Λ^{-2}	Λ^{-4} $[\Lambda^{-2}]$	Λ^{-4} $[\Lambda^{-2}]$
C_{tu}^{1}, C_{td}^{1}	Λ^{-4} $[\Lambda^{-2}]$	–	–	–	–	Λ^{-4} $[\Lambda^{-2}]$	–
C_{Qu}^{8}, C_{Qd}^{8}	Λ^{-2}	–	–	–	–	Λ^{-2}	–
C_{tq}^{8}	Λ^{-2}	–	–	–	–	Λ^{-2}	Λ^{-2}
C_{Qu}^{1}, C_{Qd}^{1}	Λ^{-4} $[\Lambda^{-2}]$	–	–	–	–	Λ^{-4} $[\Lambda^{-2}]$	–
C_{tq}^{1}	Λ^{-4} $[\Lambda^{-2}]$	–	–	–	–	Λ^{-4} $[\Lambda^{-2}]$	Λ^{-4} $[\Lambda^{-2}]$
$C_{\phi Q}^{-}$	–	–	–	Λ^{-2}	–	Λ^{-2}	–
$C_{\phi Q}^{3}$	–	Λ^{-2}	Λ^{-2}	Λ^{-2}	Λ^{-2}	–	–
$C_{\phi t}$	–	–	–	Λ^{-2}	–	Λ^{-2}	–
$C_{\phi tb}$	–	Λ^{-4}	Λ^{-4}	Λ^{-4}	Λ^{-4}	–	–
C_{tZ}	–	–	–	Λ^{-2}	–	Λ^{-2}	–
C_{tW}	–	Λ^{-2}	Λ^{-2}	Λ^{-2}	Λ^{-2}	–	–
C_{bW}	–	Λ^{-4}	Λ^{-4}	Λ^{-4}	Λ^{-4}	–	–
C_{tG}	Λ^{-2}	$[\Lambda^{-2}]$	Λ^{-2}	–	$[\Lambda^{-2}]$	Λ^{-2}	Λ^{-2}

Table 1. Wilson coefficients in our analysis and their contributions to top-quark observables via SM-interference (Λ^{-2}) and via dimension-6 squared terms only (Λ^{-4}). A square bracket indicates that the Wilson coefficient contributes via SM-interference at NLO QCD. All quark masses except m_t are assumed to be zero. 'Single t' stands for $s-$ and $t-$channel electroweak top production.